LABORATORY INVESTIGATIONS

Peritubular Dentin, a Vertebrate Apatitic Mineralized Tissue without Collagen: Role of a Phospholipid-Proteolipid Complex

Bat-Ami Gotliv · Arthur Veis

Abstract Peritubular dentin (PTD), a highly mineralized annular ring surrounding each odontoblastic process within the dentin, is an enigmatic component in vertebrate teeth. To characterize its structure and composition, we have coupled *in situ* scanning electron microscopic (SEM) and time-of-flight secondary ion mass spectrometric (TOF-SIMS) analysis of the surface composition of intact bovine coronal dentin with the isolation of intact PTD from hypochlorite-treated dentin and its subsequent TOF-SIMS and direct chemical analysis. The isolated PTD is shown to be a mineralized but porous structure complexed with a high-molecular mass calcium-proteolipid-phospholipid-phosphate complex, which cannot be extracted from the dentin prior to demineralization. The TOF-SIMS and direct amino acid analysis data confirm that the PTD protein is rich in glutamic acid but does not contain collagen. Phosphatidylcholine, phosphatidylserine, and phosphatidylinositol are present, along with a mannose-rich glycan and chondroitin-4- and chondroitin-6-sulfate glycosaminoglycans. PTD apatite, well described in the literature, must therefore form in this noncollagenous proteolipid-phospholipid complex without the intervention of collagen; nevertheless, as shown by SEM, the apatite is formed in small platy crystals, as in the bulk of the intertubular dentin (ITD). We hypothesize that the porous nature of the PTD and its proteolipid-phospholipid complexes may be involved in regulating communication between the ITD and internal PTD tubule fluids and the odontoblasts, similar to the involvement of such lipid complexes in neural, brain,

and nuclear transport functions. Thus, the PTD should not be considered solely as a passive structural element in some teeth but as part of the system that allows for the vital function of the dentin.

Keywords Peritubular dentin · Collagen · Phospholipid · Mineralization · Scanning electron microscopy · Time-of-flight secondary ion mass spectrometry

Vertebrate tooth dentin is a dense fibrillar collagenous matrix which has mineralized. This mineralized matrix, the intertubular dentin (ITD), is permeated by a system of channels or tubules that originated as the spaces occupied by the odontoblastic process of each odontoblast as it retracted from its original position at the dentinoenamel junction (DEJ) while secreting the ITD. Most studies of dentin relate primarily to the mineral and protein structures and components of the ITD. However, in some vertebrate teeth a second phase of mineralized tissue forms within the tubule as a heavily mineralized annulus or collar, called the "peritubular dentin" (PTD), surrounding an open central channel within each tubule for a portion of its length [1]. In spite of a number of studies over many years, the nature and composition of the PTD are much less understood than those of the ITD.

After dentin formation has begun and the odontoblast pulls away from the DEJ, the main cell process fills the entire space within the tubule, surrounded by an extracellular meshwork of type I collagen fibrils and noncollagenous proteins, including phosphoproteins, glycoproteins, and proteoglycans, forming the unmineralized predentin (PD). At a particular distance from the main cell body the mature mineralized dentin matrix forms. At this point, additional extracellular matrix (ECM) proteins such as

B.-A. Gotliv · A. Veis (✉)
Department of Cell and Molecular Biology, Feinberg School of Medicine, Northwestern University, 303 E. Chicago Avenue, Chicago, IL, 60611, USA
e-mail: aveis@northwestern.edu

phosphophoryn are secreted from the tubule and initiate collagen fibril-related mineralization [2]. The mineralization front (MF) is an active zone at which enzymatic processing removes some of the PD proteoglycans and other mineralization inhibitors [3]. There is thus two-way traffic involving exocytotic addition and endocytotic removal of matrix components via the tubules in the region of the MF. The mineralized matrix constricts the tubule diameter at this point, and the tubule narrows to a more or less constant diameter over the range from the MF to the mantle dentin. In mature human dentin, the cell process remains within the tubule for about one-third of the distance from the PD toward the DEJ [4]. The PTD forms around the process.

The mineral content of human permanent tooth PTD was found to be ∼35% higher compared to the mineral content in the ITD on the basis of the weight percent Ca content, while both had a Ca/P ratio of 2.04, indicating little difference in the nature of the mineral phase [5]. More recently, electron microscopic examination of human PTD, including three-dimensional image reconstruction and electron diffraction, showed the crystals of PTD to be very similar in size and organization to crystals in the adjacent ITD [6]. Thus, it was argued that crystallization within the PTD was mediated by a collagenous matrix interaction as in the ITD. This was supported by Fourier transform infrared microspectroscopic studies of the organic and mineral components of horse PTD matrix [7], which indicated that although the organic matrix was less abundant than the ITD matrix, it was also mainly composed of collagen. However, direct isolation of human coronal PTD by density gradient fractionation prior to hydrolysis and amino acid analysis [6] showed it to be virtually free of collagen but rich in a phosphorylated, acidic protein component. Goldberg et al. [8] showed that a fine network of "amorphous material" formed in the PTD. Several studies comparing the mechanical properties of PTD and ITD have all concluded that the PTD is more spatially homogenous than the collagen fibril-based ITD. Thus, the PTD has different elastic properties [9], optical anisotropy [10], and fracture properties [11] that mark the different mechanical and structural properties of these intimately associated mineralized dentin structures.

Time-of-flight secondary ion mass spectroscopy (TOF-SIMS) is a method for mapping the composition of a surface using an intense but focused beam of heavy metal ions to eject atoms or molecular fragments from a defined surface then identify the fragments by sweeping them into a mass spectrometer. The mapping is achieved by rastering the beam over the surface. Both positive and negative fragments can be detected. All ejected species are swept into the mass spectrometer; one then selects the mass/charge (m/z) ratio for a particular component and plots the relative intensity of that m/z ratio over the surface. Our previous TOF-SIMS study [12] of intact bovine dentin surfaces revealed differences in mineral ion and organic fragment compositions of the PTD and the ITD and suggested that the bovine PTD was indeed essentially free of collagen. We had also developed procedures to partially isolate human PTD from human ITD [6]. Bovine molars are large and readily available and have an abundant PTD structure. It thus seemed appropriate to refine and apply the PTD isolation procedure to bovine teeth and to use the TOF-SIMS data to guide a more in-depth analysis of the PTD structure and composition. We report here on the nature of the bovine PTD organic matrix and, based on these data, speculate on the potential mineralization processes in this noncollagenous system.
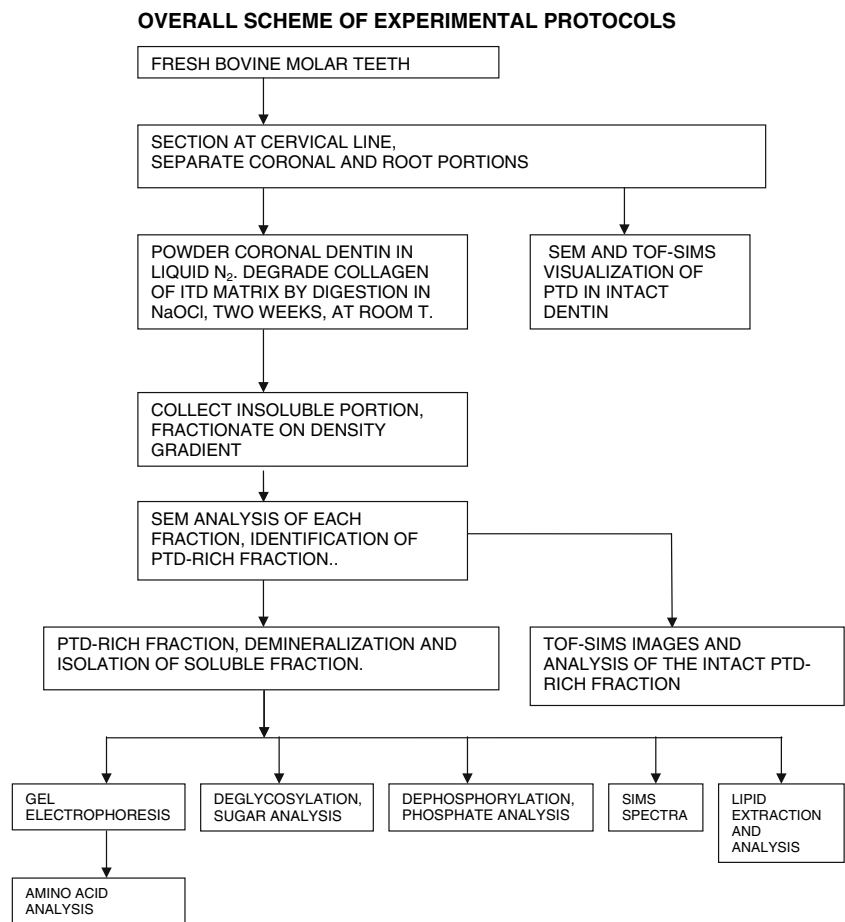
Materials and Methods

Tooth Collection and Storage

Bovine molar teeth were obtained from freshly collected mandibles of animals 12–18 months old (Aurora Packing Company, Aurora, IL). At this growth stage the mandibles contain both erupted and unerupted teeth. The jaws were placed in ice immediately upon collection and the teeth removed on the same day from their bony crypts; as described previously [12], the teeth were washed repeatedly in cold phosphate-buffered saline (PBS) solution containing 5% penicillin-streptomycin-amphotericin solution. The unerupted molars, never exposed in the animal to the oral environment, were stored before use at −80°C in PBS containing 50% glycerol. The environmentally exposed erupted teeth were washed at room temperature overnight in 5% NaOCl (Sigma-Aldrich, St. Louis, MO), then washed extensively with pyrogen-free deionized water before storage in PBS + 50% glycerol. The objective of this first NaOCl treatment was to oxidize and remove the unprotected oral cavity surface organic debris. Before freezing, the erupted teeth were sectioned near the cervical line, the root-coronal junction, using a diamond saw (Isomet 1000; Buehler, Lake Bluff, IL). The coronal and root parts were treated separately. When retrieved from storage, the teeth or sections were rinsed in deionized water to remove the glycerol.

Analysis of Structure and Composition

A flowchart correlating all of the preparative, analytical, and structural studies is presented in Fig. 1. The strategy was to separate coronal and root dentin since they have different amounts of PTD [12] and to use SEM and TOF-SIMS analyses to characterize the intact structures. Then, on the premise that the organic matrix of the more highly

Fig. 1 Flowchart for collection, preparation, and analysis of the intact PTD and its various fractions after demineralization

OVERALL SCHEME OF EXPERIMENTAL PROTOCOLS

```
┌─────────────────────────────────────┐
│ FRESH BOVINE MOLAR TEETH             │
└─────────────────────────────────────┘
                  │
                  ▼
┌─────────────────────────────────────┐
│ SECTION AT CERVICAL LINE,            │
│ SEPARATE CORONAL AND ROOT PORTIONS   │
└─────────────────────────────────────┘
          │                    │
          ▼                    ▼
┌──────────────────────┐  ┌──────────────────┐
│ POWDER CORONAL DENTIN │  │ SEM AND TOF-SIMS │
│ IN LIQUID N₂. DEGRADE │  │ VISUALIZATION OF │
│ COLLAGEN OF ITD MATRIX│  │ PTD IN INTACT    │
│ BY DIGESTION IN NaOCl,│  │ DENTIN           │
│ TWO WEEKS, AT ROOM T. │  └──────────────────┘
└──────────────────────┘
          │
          ▼
┌──────────────────────┐
│ COLLECT INSOLUBLE     │
│ PORTION, FRACTIONATE  │
│ ON DENSITY GRADIENT   │
└──────────────────────┘
          │
          ▼
┌──────────────────────┐
│ SEM ANALYSIS OF EACH  │
│ FRACTION,             │
│ IDENTIFICATION OF     │
│ PTD-RICH FRACTION..   │
└──────────────────────┘
       │            │
       ▼            ▼
┌──────────────────────────┐  ┌──────────────────┐
│ PTD-RICH FRACTION,        │  │ TOF-SIMS IMAGES  │
│ DEMINERALIZATION AND      │  │ AND ANALYSIS OF  │
│ ISOLATION OF SOLUBLE      │  │ THE INTACT PTD-  │
│ FRACTION.                 │  │ RICH FRACTION    │
└──────────────────────────┘  └──────────────────┘
```

| GEL ELECTROPHORESIS | DEGLYCOSYLATION, SUGAR ANALYSIS | DEPHOSPHORYLATION, PHOSPHATE ANALYSIS | SIMS SPECTRA | LIPID EXTRACTION AND ANALYSIS |

| AMINO ACID ANALYSIS |

mineralized, lower-collagen content PTD was both less accessible and more resistant to hypochlorite degradation, the teeth were ground to a coarse powder and given an extended exposure to a sodium hypochlorite solution, which could degrade the exposed collagen fibers of the ITD while not degrading the matrix of the PTD. In fact, as shown below, the PTD remained in tubular form after the partial removal of the ITD matrix. The mixture of partially degraded, still mineralized dentin was fractionated in a stepwise density gradient, to separate the PTD from the less mineralized, partially degraded ITD collagens and other ECM components; and the more dense apatite crystals were freed from all matrix. The various fractions were analyzed by SEM and SIMS analyses, which identified the PTD. The PTD fraction was collected and examined by SIMS and SEM. Then, the PTD fraction was demineralized, and a variety of analytical procedures were applied to determine its composition. The details and protocols are provided below.

Preparation of Isolated, Intact PTD

After washing the coronal dentin in deionized water, it was frozen in liquid N_2 and ground to a powder using a mortar and pestle. About 1 g was dispersed in 15 mL of 5 wt% NaOCl solution and stirred for 2 weeks at room temperature. The NaOCl solution was replaced by fresh solution after 1 week. The remaining mineralized dentin powder was collected by centrifugation, and 10 mL of fresh NaOCl was added. This mixture was cooled on ice and sonicated in a Heat Systems Sonicator (model 2015 Ultrasonic Processor XL; Misonix, Farmingdale, NY) at amplitude level 3 for 1 hour.

The disrupted, sonicated, mineralized dentin was fractionated in a stepwise density gradient system based on an aqueous sodium polytungstate $(2Na_2WO_4 \cdot 9WO_3 \cdot H_2O)$ solution, density 2.89 g/mL (Geoliquids, Prospect Heights, IL) as described previously [6], with only minor modifications. Five solutions were prepared and 5 mL of each layered in 50 mL centrifuge tubes: layer E, 2.664 g/mL; layer D, 2.474 g/mL; layer C, 2.278 g/mL; layer B, 2.159 g/mL; and layer A, 1.910 g/mL. Ten milliliters of the hypochlorite-sonicated dentin suspension was layered on top of layer A (60% polytungstate). The stepwise gradient was centrifuged at 2,400 rpm for 1 hour at 4°C in a Beckman (Fullerton, CA) J2-21 centrifuge with a JA-20 rotor. The mineralized particles accumulating at the appropriate density boundaries were collected. The

contents of each layer were diluted with deionized water in a separate 50 mL centrifuge tube and, after vortexing, centrifuged at 2,000 rpm for 5 minutes. This washing step was repeated five times. The final insoluble material in each fraction at the end of this process was stored at −80°C. For control purposes, dentin powder which had not been subjected to hypochlorite treatment was sonicated and separated in the polytungstate gradient system, and those fractions were washed and collected as described.

SEM Analysis

A portion of each fraction was suspended in a small volume of deionized water, and an ∼0.5 μL drop was mounted on an SEM pin using adhesive carbon tape. After drying and coating with a 6 nm layer of gold, the samples were examined in a Hitachi (Tokyo, Japan) S-3500 SEM in the high vacuum mode.

SIMS Images

After identification in the SEM, the PTD-rich fractions were mounted on magnetic discs using adhesive copper tape (SPI, West Chester, PA) and then observed in TOF-SIMS (PHI THRIFT III; Physical Electronics, Chanhassen, MN) without coating. The primary ion source was liquid gallium, producing a 25 keV ion beam. Prior to collecting spectra for analysis, the sample surface (300 μm) was cleaned by sputtering with the Ga^+ ion beam for 1 minute. The spectra were then acquired over an area of 30 x 30 μm under static conditions, detecting both positive and negative secondary fragment ions. The mass scales of the positive ion spectra were calibrated using $CH3^+$, $C2H^+$, and $C3H5^+$; the negative ion spectra were calibrated using CH^-, OH^-, and $C2H^-$. The amino acid fragment ions were identified according to their mass as determined in several studies of individual poly-amino acids adsorbed to artificial substrates [13–15]. The fragments used for imaging were selected from the fragments most unique to specific amino acids and/or yielding high signal intensity in earlier studies. Fragment ions from phospholipids were identified according to Ostrowski et al. [16]. The pertinent ion fragment masses are listed in Table 1.

PTD Demineralization

The insoluble powder collected in each density gradient fraction was demineralized in 10 mL 0.8 M HCl at 4°C overnight with agitation. The highest density fraction (fraction E) contained insoluble material, which was separated from the soluble part by centrifugation (3,000 rpm, 10 minutes). Other demineralized fractions contained only soluble materials. The soluble fractions were dialyzed against deionized H_2O overnight with three solution changes (Spectra/Por membrane MWCO = 3500; Spectrum Laboratories, Ranch Dominguez, CA). Each fraction was then lyophilized and dissolved in 1 mL dH_2O and the aliquots were stored at −20°C.

Characterization of Soluble Proteins

Sodium Dodecyl Sulfate-polyacrylamide Gel Electrophoresis (SDS-PAGE) Analysis

Precast acrylamide gels (Bio Rad Laboratories, Hercules CA) 5%, 7.5%, or 10% Tris-HCl were run under reducing conditions with 2-mercaptoethanol as the reducing agent. Staining was with Stains All silver stain (Bio Rad Laboratories, Hercules CA), using the method [17] adapted to acidic proteins [18]; Coomassie brilliant blue R250; or malachite green [19]. Malachite green-stained gels were immersed in 1% sodium bisulfite in 2 M HCl for 5 minutes and then washed in dH_2O until the background was removed.

Agarose/Polyacrylamide Gel

Mini-gel glass plates were siliconized overnight with AquaSil siliconizing fluid (Pierce, Rockford, IL) and then washed with dH_2O. Gels comprised of 1% agarose/1.2% polyacrylamide were prepared according to the procedure of Varelas et al. [20] and stained with 0.2% toluidine blue in 0.1 M acetic acid (Sigma-Aldrich).

Amino Acid Analysis

Extracts from the demineralized PTD-rich fractions were run on 10% SDS-acrylamide gels with six lanes. One lane was cut and stained with Stains All, and the position of the characteristic heavily stained high-molecular weight band [6] was determined. The remaining five unstained lanes (10 μL in each well) were cut at the position of the stained band. Amino acid. analysis of the combined gel bands was performed at the Macromolecular Structure Core Facility, Michigan State University (East Lansing, MI). The gel pieces were extracted three times with water:acetonitrile (90:10) for 1 hour with sonication. The supernatants were dried, hydrolyzed in vapor phase for 24 hours at 110°C with 5.7 N HCl, and then analyzed with the Hitachi L 8800 amino acid analyzer, using 0.3 μm Hitachi custom ion exchange resin and ninhydrin detection.

Table 1 Peaks selected for analysis of dentin surfaces by TOF-SIMS

Component	Abbreviation	Fragment/ion detected	Mass units
Mineral cations and amino acid fragment ions			
Hydroxyproline	Hyp	$C_4H_8NO^+$	86.06
Proline	Pro	$C_4H_6N^+$	68.05
Methionine	Met	$C_2H_5S^+$	61.01
Glycine	Gly	CH_4N^+	30.03[a]
Alanine	Ala	$C_2H_6N^+$	44.05[b]
Aspartic acid	Asp	$C_3H_6O_2N^+$	88
Glutamic acid	Glu	$C_3H_4O^+$	56
Serine	Ser	$C_3H_3O_2^+$	71
Ca	Ca^{2+}	Ca^{2+}	40.08
Mg	Mg^{2+}	Mg^{2+}	24.3
Na	Na^+	Na^+	23
K	K^+	K^+	39.3
Selected phospholipid-positive ion fragments			
Phospholipids (common)			165
Phospholipids (common)		$C_8H_{15}O_2^+$	143
Phospholipids (common)		$C_2H_6PO_4^+$	125
Phosphatidylcholine	PC	$C_5H_{12}N^+$	86.1
Phosphatidylcholine	PC	$C_5H_{15}NPO_4^+$	184
Phosphatidylethanolamine	PE	$C_2H_7NPO_3^+$	124
Phosphatidylethanolamine	PE	$C_2H_9PO_4^+$	142
Phosphatidylglycerol	PG	$C_3H_9PO_6Na^+$	195
Phosphatidylserine	PS	$C_3H_8NPO_6Na^+$	208

[a] This fragment is common to many other amino acids

[b] This is the most intense peak for both alanine and serine

Dephosphorylation

Demineralized PTD-rich fraction (630 μg protein) was incubated for 10 minutes at 37°C in 50 mM Tris-HCl in 1 mM $MgCl_2$ solution (pH 7.5). Alkaline phosphatase (Sigma-Aldrich) solution was then added (1 μL, 27 units). Half of this solution was frozen immediately at −20°C. The remaining solution was incubated overnight at 37°C, then dialyzed against 50 mM Tris-HCl in 1 mM $MgCl_2$ solution (pH 7.5) overnight with three solution changes (Spectra/Por membrane MWCO = 3500) to remove released phosphate. Fresh alkaline phosphatase was added (30 units), and the dephosphorylation reaction was continued at 37°C overnight.

Deglycosylation and Sugar Removal

Chemical Deglycosylation

Demineralized PTD (900 μg) was lyophilized and then deglycosylated using the GlycoFree chemical deglycosylation kit (Glyko, San Leandro, CA) and kit protocol, based on the use of trifluoromethane-sulfonic acid (TFMS). The After TFMS neutralization, the sample was dialyzed against dH_2O overnight and then incubated with sodium periodate (10 mM) for 6 hours at 4°C. After further dialysis against dH_2O, the sample was interacted for the second time with TFMS and then dialyzed before analysis by gel electrophoresis.

Treatment with Chondroitinase ABC (ChABC), Chondroitinase AC (ChAC), and Chondroitinase B (ChB)

Demineralized PTD (30 μg) was incubated at 37°C for 2 hours with 0.02 U of ChABC (Sigma-Aldrich) in reaction buffer containing 50 mM Tris-HCl, 60 mM sodium acetate (pH 8), and 0.02% bovine serum albumin. For ChAC digestion, 30 μg demineralized PTD was incubated at 37°C for 2 hours with 0.02 U of ChAC (Sigma-Aldrich) in reaction buffer containing 20 mM PBS and 0.01% bovine serum albumin. For ChB digestion, 0.1 U of enzyme was reacted at 37°C for 20 minutes with 30 μg demineralized PTD in reaction buffer containing 20 mM Tris-HCl (pH 7.5), 50 mM NaCl, 4 mM $CaCl_2$, and 0.01% bovine serum albumin.

Sugar, Sulfate, Phosphate, and Sialic Acid Analysis

The analyses for phosphate, sulfate, sialic acids, and sugars were performed by the Glycotechnology Core Facility of the University of California at San Diego (La Jolla, CA).

Phosphate and Sulfate Analysis

PTD-rich demineralized fractions, blank, and standards were hydrolyzed in 0.03 N HCl at 150°C for 1 hour, then sequentially dried in an oven at 100°C, pyrolyzed in an open flame for about 15 seconds, cooled to room temperature, and dissolved in H_2O in the appropriate amounts. Anion chromatography of phosphate and sulfate ions was performed on a DX 500 HPLC system using a Pac AS4-SC column (Dionex, Sunnyvale, CA). Samples were eluted with an isocratic mobile phase (1.7 mM $NaHCO_3$, 1.8 mM Na_2CO_3 at 2 mL/min for 20 minutes). A conductivity detector was used to identify and quantify the phosphate and sulfate contents in the sample.

Sialic Acid Analysis

The PTD-rich demineralized fraction was hydrolyzed with 2 M acetic acid at 80°C for 3 hours. The released material was collected by ultrafiltration through a Microcon YM10 filter and derivatized with 1,2-diamino-4,5-methylenedioxybenzene (DMB) to yield a fluorescent adduct. The DMB-derivatized material was analyzed by reverse-phase high-performance liquid chromatography (HPLC) using an Acclaim 120 C18 column (Dionex) at a flow rate of 0.9 mL/minute. The samples were eluted with a gradient of acetonitrile (8–11%) in methanol (7%) and water over 40 minutes, followed by 10 minutes at the final condition. The eluant was monitored with on-line fluorescence detection. The identification and quantitation of DMB-derivatized sialic acids were done by comparison with derivatized standards.

Monosaccharide Analysis of Neutral and Amino Sugars

PTD-rich demineralized fraction, blank, and standards were hydrolyzed in 2 N trifluoroacetic acid (TFA) at 100°C for 4 hours and then dried in a Speedvac (TFA GMI, Inc., Ramsey, MN). Methanol was added to the samples, which were then redried to remove traces of acid. The samples were redissolved in H_2O and the sugars separated by injecting the sample aliquot into the Dionex DX 500 HPLC system using the PA10 column and eluting in an isocratic mobile phase (18 mM NaOH at 1 mL/minute). The sugars were detected by pulsed amperometry detection (PAD).

Common monosaccharide standards found in vertebrate oligosaccharides (Man, Gal, Glc, GlcNAc, GalNAc, Fuc, and Xyl) were treated in parallel and used for calibration of the high performance anion exchanged-pulsed amperometric detection (HPAEC-PAD) response.

Uronic Acid Analysis

PTD-rich demineralized fraction, blank, and standards were hydrolyzed in 2N TFA at 100°C for 6 hours, dried in a Speedvac, and then dried again after methanol was added. The samples were redissolved in H_2O. An aliquot of the sample was injected into the Dionex DX 500 HPLC system using the PA1 column. The sugars were eluted in a 0–250 mM NaOAc in 100 mM NaOH gradient at 1 mL/minute for 30 minutes, monitored by PAD. Common uronic acid standards (glucuronic, galacturonic, and iduronic acids) were treated in parallel and used for calibration of the HPAEC-PAD response.

Lectin Binding

The PTD-rich demineralized fraction was applied to three different mannose binding lectin spin columns: LCH, GNA, ConA (Qproteome Mannose Glycoprotein kit; Qiagen, Valencia, CA). The flowthrough and the bound materials were analyzed in SDS-polyacrylamide gels stained with either Stains All or silver stain.

SIMS Spectra, Soluble Components

A 0.5 μL aliquot of the demineralized PTD-rich fraction solution was mounted on a silicon wafer chip (5 x 5 mm, SPI). The chip was mounted on a magnetic disc using adhesive copper tape (SPI), and the sample was allowed to dry overnight at room temperature. After sputtering and cleaning the sample surface in the TOF-SIMS (sputtering over 300 μm surface for 1 minute), spectra were collected for 10 minutes using the liquid gallium ion beam at 15 keV from three different regions of the wafer using either the SIMS positive ions mode or the negative ions mode.

The relevant fragments were identified in each spectrum according to Table 1, and the fragments were counted using the Job Wizard program, a part of the TOF-SIMS program. The average counts from the three different regions were calculated and normalized.

Lipid Extraction and Analysis

Lipids were extracted from the demineralized PTD-rich fraction using two protocols [21]. In the first method [22],
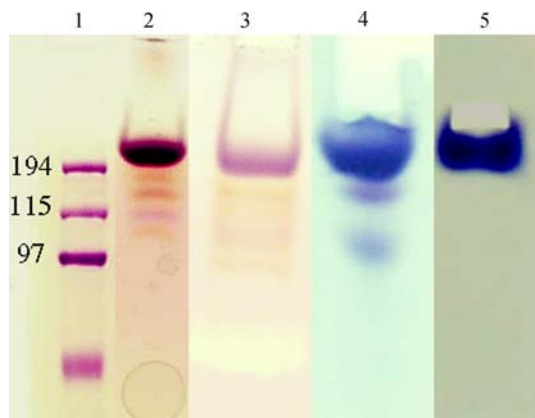
Fig. 2 Acrylamide and agarose/acrylamide gel electrophoresis of the total mineralized residue remaining after prolonged NaOCl digestion. *Lane 1*, Globular protein standards; *lane 2*, Stains All-stained 10% acrylamide gel of the total acid extract obtained after demineralization; *lane 3*, Stains All-stained 10% acrylamide gel of the total acid extract obtained after demineralization and digestion with AP; *lane 4*, 1% agarose/2% acrylamide gel of the total acid extract, stained with toluidine blue; *lane 5*, 1% agarose/2% acrylamide gel of the total acid extract, stained with toluidine blue after AP digestion

lipids were extracted with $CHCl_3$:MeOH (2:1) solution. The lipids in the $CHCl_3$ phase were washed with 0.9% NaCl at 4°C overnight with agitation. The $CHCl_3$ insoluble material containing the PTD proteins was stored at −20°C for further analysis.

The second method for lipid extraction was the Folch procedure, as modified by Bligh and Dyer [23] using an initial 1:2 $CHCl_3$:MeOH ratio. The MeOH phase contained the PTD proteins, subsequently analyzed by gel electrophoresis. The lipids were concentrated after evaporation of the $CHCl_3$ by a stream of N_2 and then redissolved in 200 μL $CHCl_3$.

Thin Layer Chromatography (TLC)

The extracted lipids were applied in 10 μL aliquots (up to 200 μL) to silica G-layered glass plates (20 x 20 cm; Fisher Scientific, Hanover Park, IL) and then chromatographed in one dimension in a solvent system consisting of either chloroform-methanol-acetic acid-water (25:15:4:2) or petroleum ether-ethyl ether-acetic acid (80:20:1). Phosphatidylserine (PS) and a phospholipid standard mixture for HPLC (lysophosphatidylcholine [LPC], phosphatidylcholine [PC], phosphatidylinositol [PI], and phosphatidyletanolamine [PE] [Sigma-Aldrich]) were applied to the TLC plate.

Lipid Detection

Iodine staining to identify fatty acids, iodoplatinate stain to identify phospholipids, and malachite green to examine phospholipids and some phosphoproteins were used as described by Goldberg et al. [24].

Hydrolysis of the Phospholipid Phosphate Bond

The demineralized PTD-rich fraction (200 μL) was incubated with 50 mM Tris-HCl buffer (pH 7.4) at 37°C for 10 minutes, and then 2 units of *Bacillus cereus* phospholipase C (Sigma-Aldrich) was added. The enzymatic reaction was carried out at 37°C for 3 hours and then stopped by adding 270 mM ethylenediaminetetraacetic acid (EDTA, pH 8). The lipids were extracted from this mixture as described above. The hydrolysis of PC, kindly provided by Prof. Jayme Borensztajn (Pathology Department, Feinberg School of Medicine, Northwestern University, Chicago, IL), was used as control. The resulting lipids were identified by TLC run with chloroform-methanol-acetic acid-water (25:15:4:2) and sprayed with iodoplatinate. The PTD phospholipids and the PC were applied to the TLC as controls before the enzymatic reaction.

Visualization of PTD in Intact Dentin

In our previous TOF-SIMS study [12], we made every effort to prepare polished mineralized sections perpendicular to the direction of the tubules. In the present work, we purposely cut and polished sections at an angle to the tubule direction so that they would have an oval, rather than circular, cross section. Since the PTD collar within the tubules was brittle, the PTD was frequently fractured by the polishing. In the places where the PTD collar was still evident, however, it could still be seen in the SEM; and since the top of the PTD collar was removed, the inner surface of the PTD could be visualized. SEM and TOF-SIMS scans were prepared and compared for such tilted surfaces using the protocols described [12].

Results

Isolated PTD

The powdered crowns from the erupted and less mature unerupted teeth were fractionated over the step polytungstate density gradient, both before and after the extended NaOCl digestion. Gel electrophoresis of the hypochlorite digested total bovine PTD protein extracted from the dentin after HCl demineralization showed a major deeply purple Stains All staining band at $M_r > 200$ kDa, with only minor lower mass bands (Fig. 2, lane 2). Treatment with alkaline phosphatase (AP, lane 3) reduced, but did not remove, the

Fig. 3 SEM and SIMS analysis of the PTD obtained after distribution over the polytungstate density gradient. (**A**) SEM, erupted tooth coronal dentin, collected in density gradient fraction D. NaOCl-treated. (**B**) SEM, unerupted tooth coronal dentin, collected in density gradient fraction D. NaOCl-treated. *White arrow* points out the very thin tubules. (**C**) SEM, erupted tooth coronal dentin, collected in density gradient fraction E. NaOCl-treated. *White arrow* points to a cross section of a PTD tubule, indicating the fact that the density gradient fractionation does not have as high a resolving power as hoped. (**D**) SEM, Unerupted tooth coronal dentin, collected in density gradient fraction E, NaOCl-treated. (**E, F**) SEM, control, erupted tooth coronal dentin, collected in density gradient fraction C. Not digested with NaOCl. (**G-J**) SIMS analysis of mineral ions and selected amino acid fragment ions, from PTD collected in density gradient fraction D from erupted coronal dentin. (**G**) Ca, (**H**) Glu, (**I**) Pro, (**J**) Met. Pro is characteristic for collagen, Met represents noncollagenous proteins. Note that the scale bars in each panel may represent different lengths
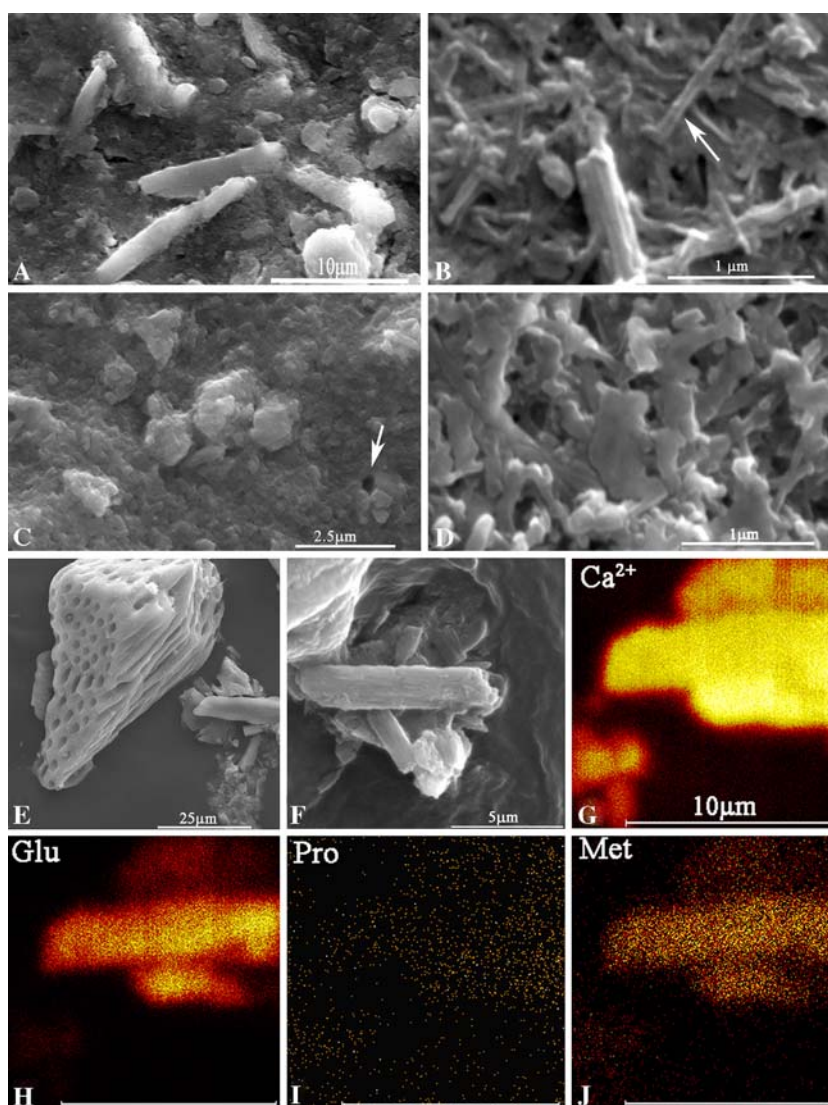
purple staining and showed no major change in complex size. Agarose/acrylamide gel electrophoresis showed the PTD protein as a strong but dull blue band (lane 4) after staining with toluidine blue (a metachromatic stain) to show acidic polysaccharides. Treatment with AP showed that the phosphate removal led to intensification of the band to a brighter blue color, indicating that acidic polysaccharides were probably present (lane 5). Thus, the mineralized bovine dentin residue after hypochlorite digestion still retained phosphorylated proteins and some acidic polysaccharides that had been protected by the mineral phase from total degradation and removal.

After distribution of the mineralized hypochlorite-digested powder over the polytungstate step gradient, the major accumulation of PTD was in fraction D, at the D-E boundary for the erupted and unerupted molars. The washed coronal fractions were all examined by SEM and TOF-SIMS before demineralization. The SEM data

showed that tubules from the erupted teeth, gradient fraction D (Fig. 3A), were thicker and evidently more highly mineralized than the very much thinner PTD (white arrow) isolated from the unerupted teeth (Fig. 3B). The most dense fractions collected in E, in both the erupted (Fig. 3C) and unerupted (Fig. 3D) teeth, were platy crystal aggregates. The platy crystals were larger in the erupted molars than in the unerupted molars. The tubular fragments observed from fraction D were clearly PTD-related since the positive ion mapping by SIMS (Fig. 3G-J) showed the main mineral ion to be Ca (Fig. 3G) and the most prominent amino acid fragment ion to be Glu (Fig. 3H), while the prominent ITD fragment ion for Pro (Fig. 3I), related to collagen, was much reduced whereas Met (Fig. 3J), indicative of noncollagenous protein, was more intense. Other mineral ions, Na, K, and Mg, were also prominent in the spectra. SIMS showed that they were very low in organic components. Having verified that the tubular
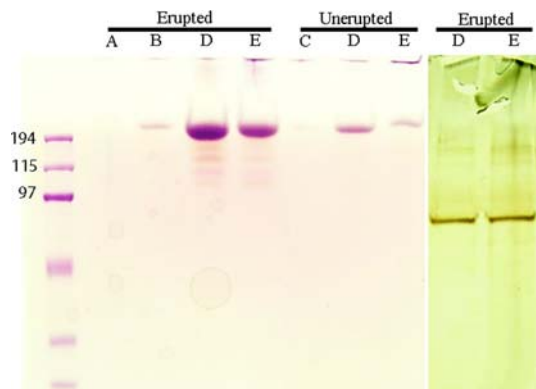
Fig. 4 Gel electrophoresis of protein components of the density gradient fractions. (*Left*) Fractions from the erupted and unerupted molars, Stains All-stained. (*Right*) Fractions from the erupted molars, silver-stained. The unerupted PTD fractionation yielded stain patterns that were similar but much less intense

Table 2 Amino acid composition of PTD fraction D soluble protein

Amino acid	Mole%
Asp	6.8
Glu	13.3
Ser	7.5
Gly	12.7
Pro	8.1
His	3.3
Thr	<0.1
Arg	4.3
Ala	6.4
Val	6.1
Met	2.4
Ile	6.2
Leu	8.4
Lys	6.0
Phe	5.8
Tyr	2.6

Table 3 Sugar, phosphate, and sulfate analyses

Component	nmole/100 μL
Sialic acid	0.022
N-Acetylglucosamine	0.04
Fucose	0.25
Galactose	0.97
Mannose	3.74
Glucuronic acid	4.13
PO_4[a]	27.435
SO_4[b]	2.56

[a] Phosphate/sulfate mol ratio = 10.72

[b] Phosphate/serine mol ratio = 12.35 (serine determined from Table 1 data)

structures captured in density gradient fraction D had the SIMS signature seen in the PTD of the intact dentin, it was concluded that density fraction D was appropriate for more detailed analysis of the PTD components. The density gradient distribution of the control dentin which had not been subjected to the prolonged collagen degradation with NaOCl yielded the major fraction as retained by the C-D density boundary. SEM (Fig. 3E, F) showed that fraction to contain large aggregates of tubules, still containing some ITD matrix that binds them together, consonant with the higher collagen content and lower density of these larger particles.

The collected fractions from each layer were demineralized and the soluble components subjected to gel electrophoresis. As shown in Fig 4, the major PTD protein in both the erupted and unerupted teeth was present in the fraction retained at the D-E boundary, hereafter called "PTD-D." The concentration of the PTD-D was greatest in the erupted coronal dentin. The fractionation was not complete as some of the platy protein PTD-E fraction also contained some PTD-D tubular fragments, as shown in Fig 3C (white arrow). The Stains All-stained protein did not stain with Coomassie blue or silver, but silver staining showed the presence of another component with an apparent size of ≤ 95 kDa in both PTD-D and PTD-E.

Root dentin treated with NaOCl provided only a small yield of PTD particles, and after demineralization, electrophoresis of the soluble protein showed much less Stains All- or silver-staining protein, even when compared to the faint staining of the unerupted coronal dentin. However, the faint bands detected (not shown) were at positions comparable to those of erupted coronal PTD-D, correlating well with our earlier observation from TOF-SIMS studies [12] that the root tubules had only a sparse PTD annulus.

Attempts to sequence the protein(s) stained with Stains All were unsuccessful. The protein band was cut directly from the gel before staining according to a prestained molecular weight marker. The proteins were digested with trypsin. HPLC separation showed well-distinguished chromatographic peaks (data not shown), but no definitive protein sequence could be obtained from these fractions.

Analysis of Composition, PTD-D

After demineralization in 0.8 M HCl and dialysis to remove the mineral ions and other low-molecular mass components, the water-soluble portion of PTD-D from a number of runs was divided into aliquots (Fig. 1), and these were subjected to a variety of analyses.

The amino acid composition data (Table 2) supported the SIMS data [12] and human PTD data [6] in showing that the PTD-D protein was essentially free of collagen (no
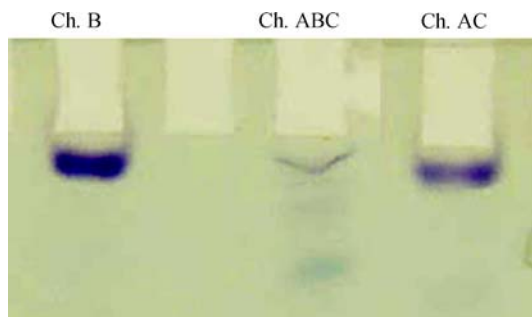
Fig. 5 Agarose gel electrophoresis after digestion of PTD by ChAC, ChB, and ChABC, toluidine blue staining. The ChABC digestion clearly reduced the total staining of the main band. Treatment with ChB, specific for the dermatan sulfate chains, reduced the staining of the intact PTD; but ChAC, specific for CS-A and CS-C, was much more effective at degrading the proteoglycans. Thus, the main glycosaminoglycans were typical ECM constituents

hydroxyproline) and relatively rich in glutamic acid, with an apparent 2/1 ratio of Glu to Asp.

The gel electrophoresis data of Fig. 2, showing only the partial removal of phosphate from the PTD-D by AP, and the toluidine blue staining of the PTD-D in the agarose-acrylamide gels suggested that the PTD-D protein might be a complex of phosphorylated protein and acidic polysaccharide. Direct analysis of phosphate and sulfate ion contents (Table 3) showed that, on a mole/mole basis, the phosphate content was approximately 11 times higher than the sulfate content. This was in agreement with the low N-acetylglucosamine content, also shown in Table 3, indicating that the PTD sulfated proteoglycan content was small. However, sulfated proteoglycans of the chondroitin 4-sulfate (CS-A), chondroitin 6-sulfate (CS-C), and dermatan sulfate (CS-B) types were present, as shown via agarose-acrylamide gel electrophoresis and toluidine blue staining, by the effects of ChAC, ChB, and ChABC on the PTD-D extract (Fig. 5). While ChABC effectively removed the majority of the toluidine blue staining, ChB alone was much less effective at reducing the staining compared to ChAC. Thus, the major sulfated glycosaminoglycans appear to be of the CS-A and CS-C types, while dermatan sulfate is present in a smaller proportion.

The high phosphate content of PTD-D cannot be accounted for by the extent of phosphorylation of the PTD-D protein. The serine content of an equivalent aliquot of PTD protein was determined from the amino acid analysis data (Table 2). These data showed that the PO_4/Ser mole ratio was 12.3. Thus, even if all possible sites in the PTD protein were phosphorylated, there is a substantial excess of phosphate moieties. The remaining data in Table 3 suggest that mannose-rich oligosaccharides are principal saccharide constituents of the PTD; however, these were not linked to protein since analysis of lectin binding showed that neither ConA, GNA, nor LCH removed any protein from the PTD-D

(data not shown). These data suggested that the excess phosphate content of the PTD might be related to the presence of membrane-type phospholipids and glycolipids, and further characterization proceeded in that direction. Removal of all the carbohydrate moieties by chemical deglycosylation did not substantially reduce the mass of the high-molecular weight PTD-D protein complex (data not shown), substantiating that the carbohydrates were not the major components of the complex.

PTD Lipids

TOF-SIMS examination of the mineralized PTD particles collected as PTD-D (Fig. 6) showed the presence of mass fragment ions corresponding to PC, $m/z = 184$ and 86.1; PE, $m/z = 124$ and 142; phosphatidylglycerol (PG), $m/z = 195.52$; and PS, $m/z = 208$; plus fragments common to all these phospholipids at $m/z = 165$, 143, and 125, all listed in Table 1. The presence of these phospholipids in PTD-D was confirmed in two ways. The PTD-D extract after HCl demineralization was run directly on gel electrophoresis and stained with malachite green before and after neutral lipid extraction by the Folch procedure. As shown in the Stains All-stained gel in Fig. 7A, the initial preparation showed the typical heavily stained, high-molecular mass protein complex even after extraction with methanol/chloroform. A small amount of material was soluble in the $CHCl_3$ phase (Fig. 7A, lane a), but the bulk of the protein was not (lane b). The malachite green stain for phosphate and phospholipids showed (Fig. 7B) the presence of phospholipids before the Folch extraction (lane a), but the staining was actually intensified in the fraction remaining after lipid extraction (lane b). The fact that malachite green stained the band strongly after the lipid extraction is an indication of the existence of inorganic phosphate complexed in the high-molecular weight band.

TLC was carried out. Distribution of the PTD-lipid fraction yielded two prominent but somewhat diffuse bands that stained with iodoplatinate, at Rfs of 1 and 0.87; but these did not match the sharper bands of the standards for PE (0.733), PC (0.633), PS (0.55), PI (0.266), or LPC (0.133). The bands with Rf = 1 were probably neutral lipids or fatty acids. The lipids with Rf = 0.87 were definitely phospholipids since these stained with idoplatinate and were removed upon treatment with phospholipase C. This diffuseness of the migrating did not permit clear identification of the particular phospholipids, probably because of the degradation of mineral-related phospholipids during extraction. In a study of the extraction of phospholipids from mineralizing growth plate cartilage matrix vesicles, Wu et al. [25] noted that the phospholipids in mineralizing matrix vesicles either complexed with the

Fig. 6 TOF-SIMS of particles of PTD-D, positive ions scanned over *m/z* ranges characteristic of phospholipids. PC, PE, PG, and PS. The shape of the particle examined is shown by the Ca- and Na-positive ion SIMS images
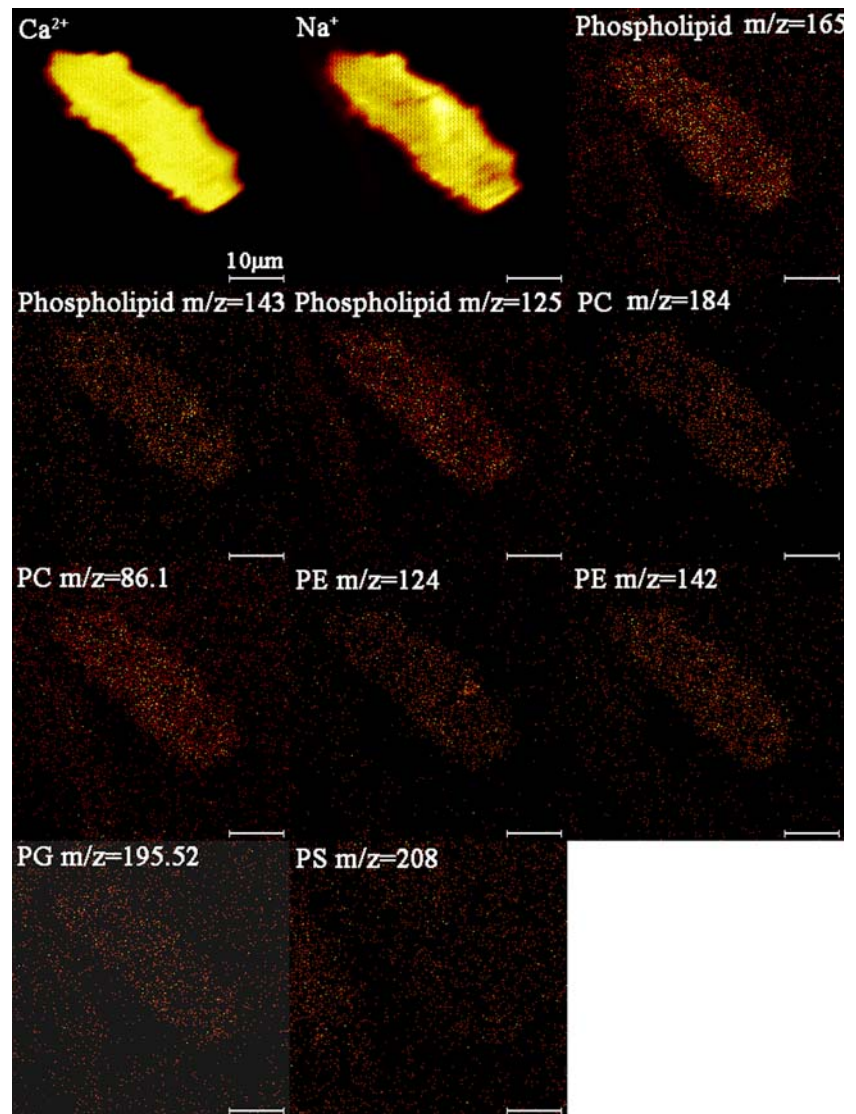
mineral or degraded rapidly during their extraction, reducing the yield. Moreover, each lipid degraded at different rates and to different extents. Further, it was found that extensive phospholipid degradation occurred during the calcification process and was accompanied by an increase in free fatty acid content. In our case, the processing problem was probably exacerbated by the extensive bleaching during processing of the dentin to collect the PTD. This suggests that the qualitative *in situ* identification of the phospholipid components as PC, PE, PG, and PS fragment ions by SIMS analysis (Fig. 6) is a more reliable measure of the *in vivo* situation.

The high-molecular weight band did not substantially change its position in the upper part of the gels upon any of the biochemical treatments described above. Even when large-pore gels were used, the complex remained at the upper part of the gel. Therefore, the putative high-molecular weight protein-phospholipid-sugar-Pi complex has a

structure or properties creating anomalous migration in the SDS-gel electrophoresis system.

SEM and TOF-SIMS Visualization of Intact PTD

Many attempts have been made to visualize the details of the intact PTD within tubules by electron microscopy, but this has been difficult for a variety of reasons, chief among which are the heterogeneity of the tubules with regard to their relative position within the dentin from the DEJ to the MF [26] and the sinuous course that the tubules take in retracting from the DEJ. For this part of the study, we selected a portion of the tooth crown wherein the tubules have a definite PTD collar but are mainly devoid of the cell processes, a position about midway between the DEJ and MF. A tilt of 35–45° appeared to provide the best retention of the PTD annulus. Figure 8A shows a group of tilted
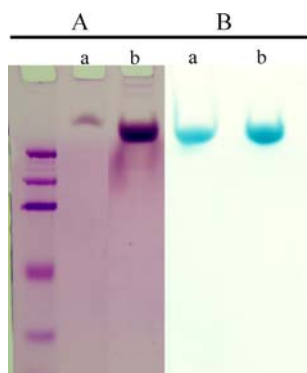
Fig. 7 Phospholipids in PTD-D. The HCl-soluble components if PTD-D before and after Folch extraction of the PTD-D particles. (**A**) Stains All staining of gel electrophoresis pattern. *Lane a*, protein recovered from the CHCl$_3$ phase; *lane b*, the protein not soluble in the CHCl$_3$ phase. (**B**) Malachite green stains of the gel electrophoresis patterns for phospholipids. *Lane a*, the total extract before Folch extraction; *lane b*, the extract after removal of the neutral lipid by Folch extraction

tubules in which the inner PTD material is partially retained (thick arrows), and in the more fortuitously cut tubule in the lower left corner the inner tubular surface is seen to have a nonfibrillar, spongy appearance. During the polishing, the fragile PTD annulus in the exposed inner surface has been partially removed from most of the tubules, showing that the ITD surrounding the tubule is

clearly collagenous. The exposed collagen fibrils (thin arrows) run circumferentially around the tubules, as shown in earlier transmission electron microscope studies [26]. TOF-SIMS mapping of a similar tilted polished section, showing the colocalization of Ca ion and either proline (Fig. 8B, lane a), hydroxyproline (lane b), or glutamic acid (lane c), demonstrated that the mineralized PTD was indeed essentially devoid of collagen but enriched in a glutamic acid-containing protein. However, in comparing the amino acid distributions in the same tubule (the centers marked with a star in Fig. 8B, lane a [Pro] and lane c [Glu]), it is clear that where the PTD has been fractured away, the inner surface of the tubule shows the presence of collagen, while the content of the Glu-rich component is reduced. These are qualitative data. The fact that the internal tubule surface is below the plane of the polished surface reduces the relative efficiency of the secondary ion scattering from the internal surface.

Discussion

Intact Dentin

The SEM and TOF-SIMS data in Figure 8A and B for the polished coronal dentin surface tilted at about 45° from the
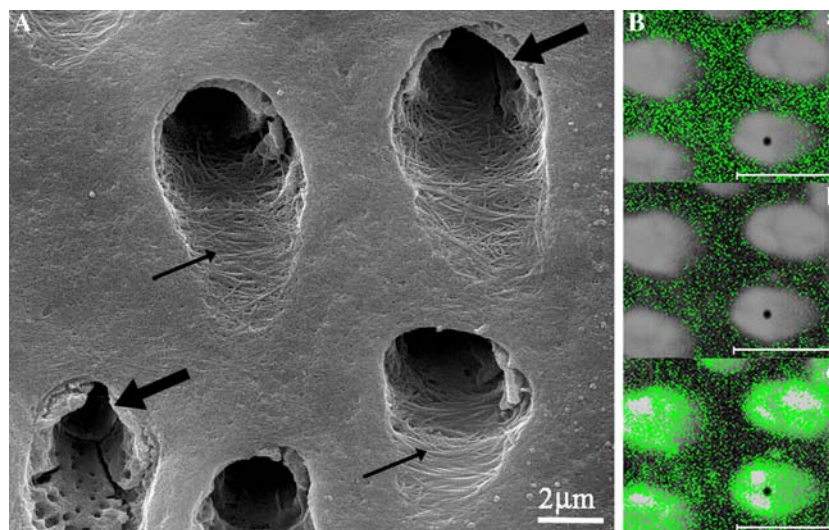

Fig. 8 (**A**) SEM of an oblique cut and polished dentin surface showing the somewhat elliptical cross sections of the cut tubules. In the majority of tubules, PTD has been mechanically fractured and removed during the polishing. The two tubules marked with *thick arrows* retain the PTD but have no central process. Note the nonfibrillar, rather spongy, porous appearance of the PTD. The internal surfaces exposed by the fragmentation of the PTD are clearly collagen fibrils (*thin arrows*). (**B**) SIMS analysis of the colocalization of Ca ion with (**a**) Pro, (**b**) Hyp, and (**c**) Glu. Comparison of the same slightly elliptical tubule (*). In these three frames, one is looking at the same set of tubules, equivalent to the SEM image on the left (**A**).

In **a** (proline) and **b** (hydroxyproline) one sees the outer surface of the PTD collar as collagen-poor, surrounded by the collagen-rich ITD. In **c** the outer surface of the PTD clearly contains a Glu-rich component colocalized with the Ca ion. Note that the Glu signals falls off in the more elliptical portion of the tubule at the area of the exposed collagen (*thin arrows*, **A**) at the inner tubule surface where the PTD collar has been fractured and removed. In this same region the Pro fragment ions from the collagen increased in intensity. However, quantitation is difficult because the inner tubule surface is at a lower level than the polished surface, rendering the secondary ion emission less intense overall

perpendicular to the tubule direction clearly show that the PTD is a separate phase that forms a distinct annulus within each tubule. At the level where this surface was cut, the central cores of the annuli appear empty, free of the odontoblastic processes originally present. The annular rings appear to be perforated by many small channels (thick arrow, Fig. 8A), probably allowing passage of any diffusible components within the tubule or ITD across the PTD. Thus, it appears that the PTD does not cut off communication between the ITD and the fluid within the tubule and its odontoblast process. As noted many times before [27], the collagen fibrils of the ITD run circumferentially around the tubules (thin arrows, Fig. 8A). The *in situ* surface analysis of the component composition by the TOF-SIMS technique (Fig. 8B) qualitatively confirms the fact [12] that the list of organic components of the PTD does not include collagen. The PTD does contain components more representative of noncollagenous proteins, with a high content of glutamic acid residues relative to aspartic acid. The situation is thus the opposite of the Asp/Glu >1 ratio in the most prominent ITD noncollagenous proteins. The lack of fibrillar proteins in the PTD and its apparent brittleness and ease of fracture are in agreement with earlier studies [9–11] showing the PTD to have distinctly different mechanical properties from the ITD.

Dentin can be isolated, frozen in liquid N_2, and crushed to a fine powder; but the powder cannot be fractionated very well by density into ITD and PTD because of the intimate and tight wrapping of the PTD with the collagen fibrils (Figs. 3E, F and 8A). On the basis that the mineralized ITD collagen might nevertheless be more accessible and hence preferentially removed by oxidation with prolonged treatment with NaOCl, a technique used by those studying shells of various types to remove the intercrystalline organic sheaths around the crystal plates, the mineralized dentin powders were digested. The remaining particles recovered after digestion were found to contain an essentially acidic protein (Table 2) and after demineralization to yield a soluble, very high-molecular mass component (Fig. 2, lane 2) that stained intensely with Stains All but only faintly with silver stain or Coomassie. Treatment with AP (lane 3) clearly removed a portion of the staining but did not markedly lower the apparent molecular size. Toluidine blue staining of the PTD component (in an agarose/acrylamide gel) yielded strong staining for acidic protein and glycosaminoglycans (lane 4), but surprisingly, AP treatment (lane 5) showed an intensification of the toluidine blue staining, suggesting that the phosphoproteins present may have blocked the initial staining.

The density gradient fractionation of the NaOCl-treated coronal dentin was very different for the erupted and unerupted teeth in that the mature teeth had more heavily mineralized PTD than the less mature unerupted teeth. The tubular structures obtained as PTD-D (Fig. 3A) were almost ten times longer and thicker than the corresponding PTD-D fraction from the unerupted molars (Fig. 3B). The platy crystals of PTD-E are also presented at different magnification in Fig. 3C, D. The corresponding TOF-SIMS surface analysis of a representative fragment from mature coronal PTD-D (Fig. 3G-J) show them to be heavily mineralized, with Glu as the most prominent amino acid fragment. The Pro signal was quite low, and Hyp (not shown) was near background level. The SIMS scan presentations in the form given are qualitative in terms of absolute concentration, but the color intensities in each scan are normalized to the highest intensity signal. Thus, the well above background localization of Glu and Met (indicative of noncollagenous proteins) to the same positions as the Ca ion in contrast to the Pro and, more so, the Hyp signals, which were almost uniform across the same scanned field, showed the distinction between the PTD protein and the collagen of the ITD.

As shown in Fig. 4, the PTD-D fractions from the erupted molars showed a much higher concentration of the Stains All staining band at $M_r > 200$ kDa than that from the unerupted teeth, and the higher amount of protein in the erupted PTD-D allowed visualization of a silver-stained band at $M_r < 97$ kDa. Minor bands were present in both Stains All- and silver-stained gels, showing that several proteins are present in each. Although the NaOCl treatment leaves these proteins in the mineral phase, it is possible that some degradation also occurs and that these minor components may be artifactual products of the processing. The oxidative degradation may not be too harsh, however, since the compositional analyses (Table 3) show that glycosaminoglycans and a mannose-containing oligosaccharide are present. While the sulfate analysis is quantitatively consistent with the presence of chondroitin sulfate proteoglycans (Fig. 5), the total high phosphate content cannot be correlated with either the Ser content of the proteins or the putative phosphorylated sugars. Gel electrophoresis of PTD-D extract followed by staining with malachite green showed the presence of phosphate and phospholipids (Fig. 7B).

The characterization data presented here make it quite clear that the mineralized peritubular dentin is a complex mixture of an acidic protein, phospholipid, or possibly proteolipid complex, with small amounts of glycoproteins and proteoglycans. However, there are some formidable questions remaining for characterization. It is still necessary to learn how to disaggregate the complex and isolate the individual proteins for sequencing and to determine the amounts of free and covalently bound phosphate present and what is responsible for the insolubility of the complex.

It has been known for a long time [28–30] that lipids are present in dentin and bone, and many have suggested that

they have an important role in mineralization. Interest has focused on matrix vesicles [31], extracellular lipid bilayer-enclosed vesicles whose membranes are enriched in specific phospholipids relative to typical cell membrane lipid compositions [32, 33], particularly in cartilage calcification. The matrix vesicle lipids are not readily extracted from mineralized tissues, and recently Wu et al. [25] showed that extensive phospholipid degradation could occur during matrix vesicle calcification so that the composition of the extracted lipids and their extractability changed during calcification. Matrix vesicles, however, are not prominent in dentin, appearing only in the earliest stages of mantle dentin formation. Yet, phospholipids of composition similar to that found in matrix vesicles, bone, and dentin seem to be present in the PTD.

The high-molecular weight lipid-containing complexes found in the PTD-D fraction are also strikingly similar to the calcium-phospholipid-phosphate complexes with proteolipid isolated from the calcifying bacteria *Bacterionema matruchoti* [34], which consisted of 52 mole% Ca, 32 mole% organic phosphate, and 15 mole% inorganic phosphate. The phospholipids were a mixture of PI, PI-4-phosphate, PI-4,5-diphosphate, and PS. These complexes were very difficult to dissociate. Their proteolipid protein component has not been identified or characterized. However, a presumably similar proteolipid isolated from *Corynebacterium matruchotii* after dissociation from phosphoproteins, other lipids, and Ca complexation has been cloned and sequenced by van Dijik et al. [35]. The protein portion of this proteolipid was calculated to be only ∼5.5 kDa and had an isoelectric point of 4.28. Phospholipid-proteolipid complexes have been studied in the brain [36], and recently [37] they have been shown to have important roles in proper neurological function. Phospholipid-proteolipid complexes are present in cell nuclei from all cell types but are not in the nuclear envelope as part of the bilayer membrane. They may be involved in many signaling activities [38]. Thus, the Ca-phospholipid-proteolipid complexes are ubiquitous and reactive in many signaling and ion transport processes. These observations led us to suggest that the PTD may also have direct roles in some active transport, regulatory activities related to keeping the coronal dentin a live and vital tissue throughout tooth life.

These considerations suggest that we should take a rather different approach to understanding the role of the PTD, that of participating in the communication between the vital dentin ECM and the vital odontoblasts, rather than to its being restricted to a passive structural role.

References

1. Goracci G, Mori G, Casa de'Martinis L, Bazzucchi M (1993) Analisi ultrastructurale della dentina peritubulare e del lume tubulare di denti sani. Minerva Stomatol 42:205–216

2. Rabie AM, Veis A (1995) An immunocytochemical study of the routes of secretion of collagen and phosphophoryn from odontoblasts. Connect Tissue Res 31:197–209

3. Moriguchi M, Yamada M, Yanagisawa T (1998) Immunochemistry of proteoglycan in dentin and odontoblasts. J Anat (Japan) 73:239–245

4. Goracci G, Mori G, Marci F, Baldi M (1999) Extent of the odontoblastic process. Analysis by SEM and confocal microscopy. Minerva Stomatol 48:1–8

5. Hirayama A (1990) Experimental analytical electron microscopic studies on the quantitative analysis of elemental concentrations in biological thin specimens and its application to dental science [in Japanese]. Shikawa Gakuho 90:1019–1036

6. Weiner S, Veis A, Beniash E, Arad T, Dillon JW, Sabsay B, Siddiqui F (1999) Peritubular dentin formation: crystal organization and the macromolecular constituents in human teeth. J Struct Biol 126:27–41

7. Magne D, Guicheux J, Weiss P, Pilet P, Daculsi G (2002) Fourier transform infrared microspectroscopic investigation of the organic and mineral constituents of peritubular dentin: a horse study. Calcif Tissue Int 71:179–185

8. Goldberg M, Molon Noblot M, Septier D (1980) Effect of 2 methods of demineralization on the preservation of glycoproteins and proteoglycans in the intertubular and peritubular dentin in the horse. J Biol Buccale 8:315–330

9. Kinney JH, Balooch M, Marshall SJ, Marshall GW Jr, Weihs TP (1996) Atomic force microscope measurements of the hardness and elasticity of peritubular and intertubular human dentin. J Biomech Eng 118:133–135

10. Iwamoto N, Ruse ND (2003) Fracture toughness of human dentin. J Biomed Mater Res A 66:507–512

11. Wang R (2005) Anisotropic fracture in bovine root and coronal dentin. Dent Mater 21:429–436

12. Gotliv B-A, Robach JS, Veis A (2006) The composition and structure of bovine peritubular dentin: mapping by time of flight secondary ion mass spectroscopy. J Struct Biol 156:320–333

13. Mantus DS, Ratner BD, Carlson BA, Moulder JF (1993) Static secondary ion mass spectrometry of adsorbed proteins. Anal Chem 65:1431–1438

14. Samuel NT, Wagner MS, Dornfeld KD, Castner DG (2001) Analysis of poly(amino acids) by static time-of-flight secondary ion mass spectrometry (TOF-SIMS). Surf Sci Spectra 8:163–184

15. Dambach S, Fartmann M, Kriegeskotte CCB, Hellweg S, Wiesmann H, Lipinsky D, Arlinghaus HF (2004) ToF-SIMS and laser-SNMS analysis of apatite formation in extracellular protein matrix of osteoblasts in vitro. Surface Interface Anal 36:711–715

16. Ostrowski SG, Szakal C, Kozole J, Roddy TP, Xu J, Ewing AG, Winograd N (2005) Secondary ion MS imaging of lipids in picoliter vials with a buckminsterfullerene ion source. Anal Chem 77:6190–6196

17. Myers JM, Veis A, Sabsay B, Wheeler AP (1996) A method for enhancing the sensitivity and stability of Stains-all for phosphoproteins separated in sodium dodecyl sulfate-polyacrylamide gels. Anal Biochem 240:300–302

18. Gotliv BA, Addadi L, Weiner S (2003) Mollusk shell acidic proteins: in search of individual functions. Chembiochem 4:522–529
19. Teichman RJ, Cummins JM, Takei GH (1974) The characterization of a malachite green stainable, glutaraldehyde extractable phospholipid in rabbit spermatozoa. Biol Reprod 10:565–577
20. Varelas JB, Zenarosa NR, Froelich CJ (1991) Agarose/polyacrylamide minislab gel electrophoresis of intact cartilage proteoglycans and their proteolytic degradation products. Anal Biochem 197:396–400
21. Goldberg M, Boskey AL (1996) Lipids and biomineralizations. Prog Histochem Cytochem 31:1–187
22. Wuthier RE (1968) Lipids of mineralizing epiphyseal tissues in the bovine fetus. J Lipid Res 9:68–78
23. Bligh EG, Dyer WJ (1959) A rapid method of total lipid extraction and purification. Can J Biochem Physiol 37:911–917
24. Goldberg M, Septier D, Lécolle S, Vermilen L, Bassila-Mapahou P, Carreau JP, Gritli A, Bloch-Zupan A (1995) Lipids in predentine and dentine. Connect Tissue Res 33:105–114
25. Wu LNY, Genge BR, Kang MW, Arsenault AL, Wuthier RW (2002) Changes in phospholipid extractability and composition accompany mineralization of chicken growth plate cartilage matrix vesicles. J Biol Chem 277:5126–5133
26. Takuma S (1960) Electron microscopy of the structure around the dentinal tubule. J Dent Res 39:973–981
27. Beniash E, Traub W, Veis A, Weiner S (2000) A transmission electron microscope study using vitrified ice sections of predentin: structural changes in the dentin collagenous matrix prior to mineralization. J Struct Biol 132:212–225
28. Shapiro IM, Wuthier RE, Irving JT (1966) A study of the phospholipids of bovine dental tissues. I. Enamel matrix and dentine. Arch Oral Biol 11:501–512
29. Shapiro IM, Wuthier RE (1966) A study of the phospholipids of bovine dental tissues. II. Developing bovine foetal dental pulp. Arch Oral Biol 11:513–519
30. Irving JT, Wuthier RE (1968) Histochemistry and biochemistry of calcification with special reference to the role of lipids. Clin Orthop 56:237–260
31. Bonucci E (1967) Fine structure of early cartilage calcification. J Ultrastruct Res 20:33–50
32. Peress NS, Anderson HC, Sajdera SW (1974) The lipids of matrix vesicles from bovine fetal epiphyseal cartilage. Calcif Tissue Res 14:275–282
33. Wuthier RE (1975) Lipid composition of isolated epiphyseal cartilage cells, membranes and matrix vesicles. Biochim Biophys Acta Lipids Lipid Metab 409:128–143
34. Boyan-Salyers BD, Boskey AL (1980) Relationship between proteolipids and calcium-phospholipid-phosphate complexes in Bacterionema matruchotii calcification. Calcif Tissue Int 30:167–174
35. van Dijk S, Dean DD, Liu Y, Zhao Y, Chirgwin JM, Schwartz Z, Boyan BD (1998) Purification, amino acid sequence, and cDNA sequence of a novel calcium-precipitating proteolipid involved in calcification of Corynebacterium matruchotii. Calcif Tissue Int 62:350–358
36. Zabelinskii SA, Pomazanskaia LF, Chirkovskaia EV (1984) Brain proteolipids in representatives of different vertebrate classes [in Russian]. Zh Evol Biokhim Fiziol 20:239–245
37. Turner N, Else PL, Hulbert AJ (2005) An allometric comparison of microsomal membrane lipid composition and sodium pump molecular activity in the brain of mammals and birds. J Exp Biol 208:371–381
38. Irvine RF (2002) Nuclear lipid signaling. Science's Stke: Signal Transduction Knowledge Environment 2002(150):RE13